A Genetic Strategy for the Dynamic and Graded Control of Cell Mechanics, Motility, and Matrix Remodeling

Joanna L. MacKay,[†] Albert J. Keung,[†] and Sanjay Kumar[‡*]
[†]Department of Chemical and Biomolecular Engineering and [‡]Department of Bioengineering, University of California, Berkeley, California

ABSTRACT Cellular mechanical properties have emerged as central regulators of many critical cell behaviors, including proliferation, motility, and differentiation. Although investigators have developed numerous techniques to influence these properties indirectly by engineering the extracellular matrix (ECM), relatively few tools are available to directly engineer the cells themselves. Here we present a genetic strategy for obtaining graded, dynamic control over cellular mechanical properties by regulating the expression of mutant mechanotransductive proteins from a single copy of a gene placed under a repressible promoter. With the use of constitutively active mutants of RhoA GTPase and myosin light chain kinase, we show that varying the expression level of either protein produces graded changes in stress fiber assembly, traction force generation, cellular stiffness, and migration speed. Using this approach, we demonstrate that soft ECMs render cells maximally sensitive to changes in RhoA activity, and that by modulating the ability of cells to engage and contract soft ECMs, we can dynamically control cell spreading, migration, and matrix remodeling. Thus, in addition to providing quantitative relationships between mechanotransductive signaling, cellular mechanical properties, and dynamic cell behaviors, this strategy enables us to control the physical interactions between cells and the ECM and thereby dictate how cells respond to matrix properties.

INTRODUCTION

Cells physically pull on their surroundings through actomyosin contraction, and this force is opposed in part by the mechanical resistance of the extracellular matrix (ECM) and neighboring cells. The balance between these mechanical forces is critical for maintaining tissue homeostasis and proper cell function, and changes in the mechanical properties of cells and the ECM have been implicated in the development of cancer and other diseases (1–3). The development of techniques to precisely engineer the biophysical properties of the ECM (e.g., protein micropatterning (4) and tunable-stiffness gels (5)), has led to the observation that subtle changes in matrix properties, such as stiffness and geometry, can act through mechanotransductive signaling networks to dramatically affect cell behavior (6,7). On the other side of this force balance, however, there are relatively few tools to control the mechanobiological properties of cells independently from the properties of the matrix in a precise manner. As a result, it has been challenging to develop a quantitative understanding of how changes in mechanotransductive signaling translate to changes in specific cellular mechanical properties, and how these properties influence cell-ECM interactions. Clarification of these relationships could significantly advance both our fundamental understanding of cellular mechanobiology and our ability to direct cell behavior in cell and tissue engineering applications.

Most direct manipulations of mechanobiological signaling have sought to control cytoskeletal assembly and mechanics by turning specific proteins on or off in a concerted fashion, e.g., with protein overexpression, pharmacological inhibitors, or siRNA. These approaches have been instrumental in identifying key mechanotransductive proteins, but they do not allow one to explore the effects of more measured changes in protein activity, such as those that are likely to be encountered physiologically. Surprisingly, only a handful of studies have modulated the activity of mechanotransductive proteins in these intermediate ways in living cells, primarily by varying the concentration of pharmacological inhibitors of the nonmuscle myosin II activation pathway (8–12). Such pharmacological agents, however, suffer from several important drawbacks, including a small set of available drug targets, a limited ability to activate rather than suppress those targets, relatively steep dose-response relationships, and concerns about off-target and toxic effects.

In this study, we sought to gain more precise and versatile control over the mechanobiological properties of cells by using genetic engineering techniques to vary the expression of mutant mechanotransductive proteins from a repressible promoter. We demonstrate that with a single copy of a constitutively active (CA) mutant gene placed under a tetracycline-repressible promoter, we can directly modulate a number of cellular mechanobiological properties, including cytoskeletal architecture, cortical stiffness, traction force generation, and motility, in a graded fashion. We also show that we can exert dynamic control over cell-ECM interactions on a collagen hydrogel by reversibly switching expression of the CA mutants on and off over time. By enabling graded control over protein activity and cellular force generation without the disadvantages of pharmacological inhibitors, this approach can both facilitate quantitative investigations of mechanotransductive

Submitted July 14, 2011, and accepted for publication December 19, 2011.

*Correspondence: skumar@berkeley.edu

Editor: Alissa Weaver.

0006-3495/12/02/0434/9 $2.00

doi: 10.1016/j.bpj.2011.12.048

signaling pathways and serve as a design handle for genetically instructing cell behavior at cell-material interfaces.

MATERIALS AND METHODS

Cell lines and reagents

Myc-tagged RhoA Q63L and MLCK ED785-786KK (13) were subcloned into the retroviral vector CLGPIT containing the tetracycline-repressible promoter, puromycin resistance, and green fluorescent protein (GFP) as previously described (14). Viral particles were packaged in 293T cells and used to infect U373-MG and U87-MG human glioma cells at a multiplicity of infection of 1 IU/cell. Cells were cultured in Dulbecco's modified Eagle's medium with 10% calf serum, selected with 1 μg/ml puromycin, and expanded in culture with 100 ng/ml tetracycline. At least 2 days before experiments were conducted, the culture medium was changed to 0.1% calf serum and the appropriate tetracycline concentration. The U373-MG GFP and control cell lines were created in the same manner with a single copy of GFP placed under the tetracycline-repressible promoter and no encoded gene, respectively. Blebbistatin and oleoyl-L-α-lysophosphatidic acid were obtained from Sigma-Aldrich (St. Louis, MO), and NSC23766 was obtained from EMD Chemicals (Gibbstown, NJ).

Western blots

Cells were lysed in RIPA buffer with protease and phosphatase inhibitors. Protein content was measured by BCA assay (Thermo Fisher Scientific, Rockford, IL) and normalized across samples. Lysates were boiled, run on a 4–12% Bis-Tris gel, and transferred onto a PVDF membrane (all from Invitrogen, Carlsbad, CA). As the primary antibodies, we used anti-RhoA and anti-Myc (Cell Signaling Technology, Danvers, MA); anti-glyceraldehyde-3-phosphate dehydrogenase (anti-GAPDH), anti-vinculin, and anti-myosin light chain (all Sigma-Aldrich); and anti-integrin β1 and anti-α-actinin (Santa Cruz Biotechnology, Santa Cruz, CA). HRP-conjugated secondary antibodies (Invitrogen) and enhanced chemiluminescence reagent (Thermo Fisher Scientific) were used for detection on x-ray film. Bands were quantified via the gel analysis feature in ImageJ and normalized by GAPDH content.

RhoA activity assay

To measure levels of GTP-bound RhoA, we performed a G-LISA assay (Cytoskeleton, Denver, CO) according to the manufacturer's directions.

Measurements of GFP fluorescence

An FC-500 flow cytometer (Beckman Coulter, Brea, CA) was used to measure GFP fluorescence to titer viral particles and to monitor transgene expression in the U373-MG GFP cell line.

Immunofluorescence and phase contrast microscopy

Epifluorescence and live-cell imaging were performed with a TE2000-E2 microscope (Nikon, Tokyo, Japan). Confocal imaging was performed with a BX51WI microscope (Olympus, Center Valley, PA) equipped with swept field confocal technology (Prairie Technologies, Middleton, WI). Projections of z-stacks were created in ImageJ based on standard deviations of pixel intensity. For immunofluorescence, we used the following primary antibodies: anti-focal adhesion kinase pY397 (Invitrogen), anti-N-cadherin (BD Biosciences, Franklin Lakes, NJ), and anti-vinculin (Sigma-Aldrich). F-actin and nuclei were stained with phalloidin and 4′,6-diamidino-2-phenylindole, respectively.

Traction force microscopy

Fibronectin-coated polyacrylamide gels were synthesized as previously described (14) from a 5% acrylamide and 0.2% bis-acrylamide (w/v) solution with yellow-green fluorescent microspheres (0.5 μm diameter) added before polymerization. We computed maps of cellular traction stresses from bead positions before and after cell detachment using constrained Fourier transform traction cytometry (15). We manually drew the cell outlines and used them to calculate the cell area and shape factor, which we define as $4 \times \pi \times (\text{area})/(\text{perimeter})^2$. We measured the elastic moduli of the gels for each experiment using atomic force microscopy (AFM).

AFM

Using an MFP-3D atomic force microscope (Asylum Research, Santa Barbara, CA), we indented the cells with pyramid-tipped probes (DNP or OTR4; Bruker AFM Probes, Camarillo, CA) with cantilever spring constants of 68–129 pN/nm, as measured by thermal calibration. We calculated the elastic moduli of cells from force curves using a modified Hertz model (16).

Cell migration assays

For scratch wound migration assays, cells were seeded as a monolayer, scratched with a pipette, and imaged over 6 h. The final change in wound area was averaged from at least six frames per well. We calculated the average linear speed from this change in area by dividing by time, dividing by 2 (because cells migrate inward from two sides), and dividing by the image height (to convert area/hour to distance/hour). To quantify the random motility of cells on polyacrylamide and collagen gels, we imaged the cells every 15 min for 6 h and manually tracked them using ImageJ. The polyacrylamide gel formulations and stiffness measurements were made as previously described (14).

Collagen gel contraction assay

Cells were suspended in a 1 mg/ml collagen I solution (PureCol; Advanced BioMatrix, San Diego, CA) at a concentration of 600,000 cells/ml in a multiwell plate. After 24 h, the gels were detached from the sides of the well. They were imaged 24 h later, and the change in gel area was quantified with the use of ImageJ.

RESULTS

To provide proof-of-principle that cellular mechanics can be modulated in a graded fashion through the controlled expression of mutant mechanotransductive proteins, we first targeted RhoA GTPase, a strongly validated activator of actin polymerization and actomyosin contractility (17). Using retroviral gene delivery, we introduced a Myc-tagged CA mutant RhoAQ63L under a tetracycline-repressible promoter into U373-MG human glioblastoma cells, which are highly motile and mechanosensitive (18,19). We transduced the cells at a low multiplicity of infection so that each cell would likely receive a single copy of the construct. To first confirm that we could attenuate the expression of CA RhoA in a graded fashion by adding varying amounts of tetracycline to the cell culture medium, we measured the expression levels of CA RhoA and endogenous RhoA protein via Western blot. Because the Myc tag on CA

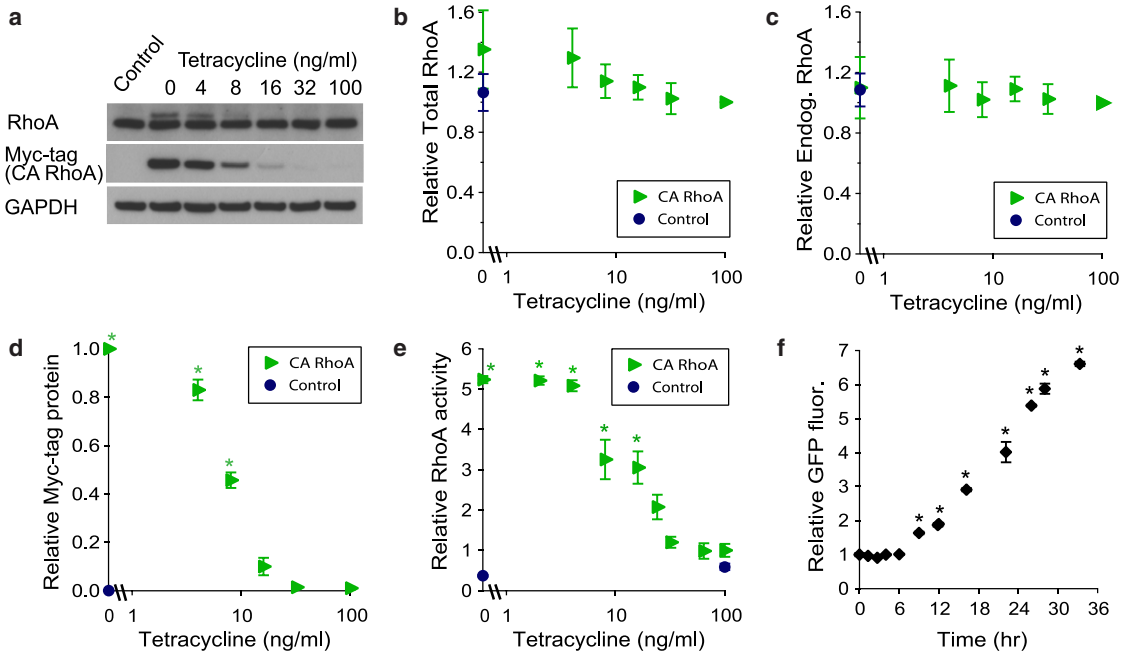

FIGURE 1 Graded and dynamic control over mechanotransductive gene expression and protein activity from a tetracycline-repressible promoter. (*a*) Western blot showing endogenous RhoA (*bottom band* of RhoA) and CA RhoA protein levels (Myc-tag and *top band* of RhoA) in U373-MG control cells and CA RhoA cells cultured in varying tetracycline concentrations. (*b* and *c*) Expression levels of total RhoA (*b*) and endogenous RhoA (*c*) were quantified relative to CA RhoA cells with 100 ng/ml tetracycline ($n = 3$ blots). (*d*) Expression levels of Myc-tagged CA RhoA were quantified relative to CA RhoA cells with no tetracycline ($n = 4$ blots). (*e*) RhoA activity of U373-MG CA RhoA and control cells measured with a G-LISA assay and displayed relative to CA RhoA cells with 100 ng/ml tetracycline ($n = 3$ samples). (*f*) Fluorescence of U373-MG GFP cells initially cultured in 100 ng/ml tetracycline, switched to tetracycline-free media, and assayed 0–53 h later. Values are relative to $t = 0$ ($n = 3$ samples). For *b–f*, mean ± SE; $*p < 0.05$ compared with 100 ng/ml tetracycline or $t = 0$ (analysis of variance (ANOVA), Tukey post-hoc test).

RhoA adds 1.2 kDa in molecular mass, we were able to visualize CA RhoA and endogenous RhoA protein as separate bands, both recognized by an anti-RhoA antibody (Fig. 1 *a*). As expected, CA RhoA expression (*top band* of RhoA) was strongest without tetracycline and decreased in a graded fashion with increasing tetracycline concentration (Fig. 1, *a* and *b*). This top band was completely absent in control cells transduced with the repressible promoter but without an encoded transgene. On the other hand, endogenous RhoA expression (*bottom band* of RhoA) did not change with tetracycline concentration (Fig. 1, *a* and *c*). With CA RhoA fully expressed (i.e., no tetracycline), we estimated that CA RhoA constitutes only 18.4 ± 0.7% of the total amount of RhoA protein ($n = 3$ blots), which translates to a 23% increase in total RhoA protein over endogenous levels. We also used an anti-Myc tag antibody to probe for CA RhoA alone, which more clearly shows the graded change in expression with tetracycline concentration (Fig. 1, *a* and *d*). To determine how these changes in CA RhoA expression translate to changes in overall RhoA activity, we measured the amount of activated (GTP-bound) RhoA in cell lysates using an ELISA-based measurement (Fig. 1 *e*). Cells cultured with 100 ng/ml tetracycline exhibited a level of RhoA activity similar to that observed in control cells, and this level increased fivefold as the tetracycline concentration was reduced. This translates to a 14-fold increase in RhoA activity over control cells, because the CA RhoA construct is somewhat leaky even at high tetracycline concentrations. To investigate the kinetics of transgene expression, we introduced GFP into U373-MG cells under the same tetracycline-repressible promoter and tracked the evolution of fluorescence intensity. After confirming that the tetracycline dose-activity relationship for GFP was similar to that observed for CA RhoA (Fig. S1 in the Supporting Material), we switched the GFP expression from off to on by washing out the tetracycline, and found that GFP fluorescence was detectable by flow cytometry within 12 h (Fig. 1 *f*).

Because RhoA is known to reinforce actomyosin stress fibers, cell-ECM adhesions, and cell-cell adhesions (20), we investigated whether we could obtain graded control over the assembly of these structures. Inducing CA RhoA expression stimulated the formation of stress fibers and active focal adhesions in a strongly tetracycline-dependent manner (Fig. 2 *a*), and treatment with the myosin inhibitor blebbistatin strongly offset this effect (Fig. S2). We found that CA RhoA expression did not alter the total protein levels of integrin $\beta 1$, vinculin, α-actinin, or myosin (Fig. S3), suggesting that this RhoA-dependent increase in active focal adhesions is likely due to changes in the localization or activation of these proteins, and not to changes in protein expression. Increasing RhoA activity

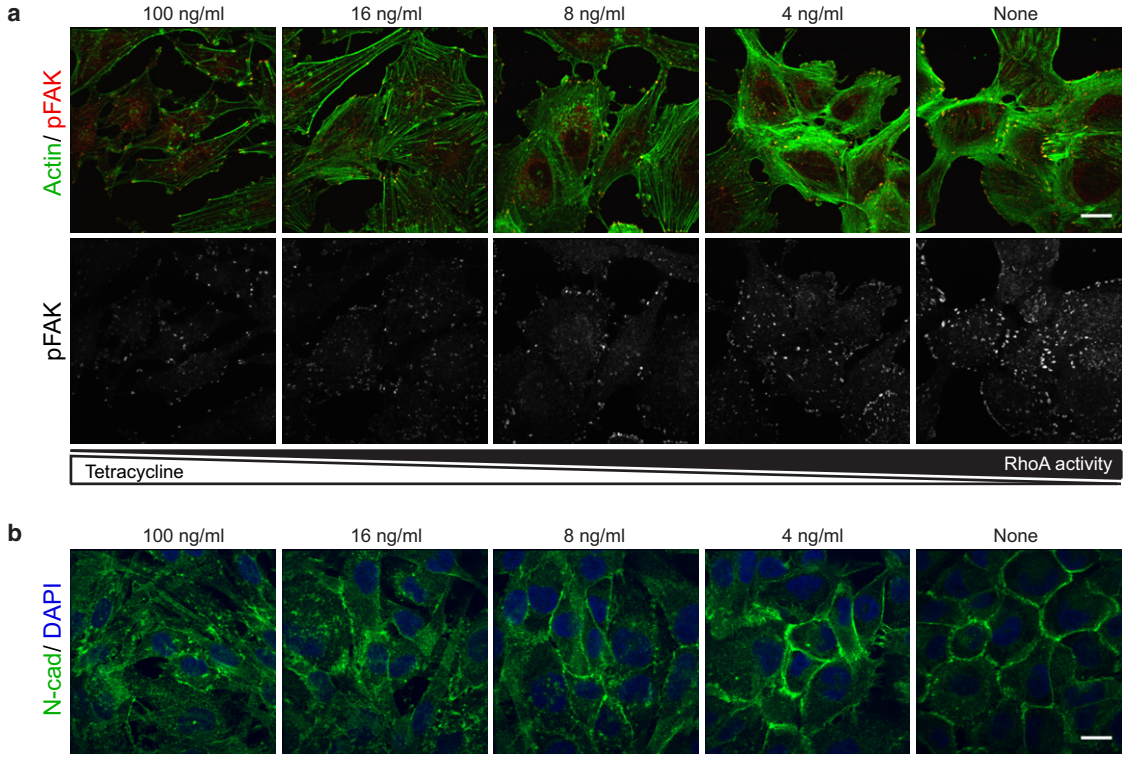

FIGURE 2 Graded formation of stress fibers, focal adhesions, and cell-cell contacts with CA RhoA expression. Confocal micrographs of U373-MG CA RhoA cells cultured in varying tetracycline concentrations before fixation and staining for (*a*) F-actin (*green*) and phosphorylated focal adhesion kinase (*red* and *second panel alone*), and (*b*) N-cadherin (*green*) and nuclei (*blue*). The top panel in *a* is a projection of z-slices. Scale bars = 25 μm.

also caused cells to adopt a less polarized morphology with better-defined cell-cell junctions, as evidenced by N-cadherin localization (Fig. 2 *b*). The cytoskeletal architecture of control cells, on the other hand, was not affected by tetracycline concentration (Fig. S4). To demonstrate graded control over stress fiber formation in a different cell line, we introduced tetracycline-repressible CA RhoA into U87-MG human glioblastoma cells and found similar effects on stress fiber and focal adhesion density (Fig. S5).

We next sought to determine whether we could use this control over RhoA activity to modulate the contractile forces that cells exert on their surroundings. Using traction force microscopy to map the traction stresses of U373-MG cells on a flexible polyacrylamide substrate, we found that the average traction stress of cells increased from 310 Pa to 510 Pa with increasing CA RhoA expression (Fig. 3 *a*). To assess whether we could achieve similar control over traction force generation through an orthogonal myosin activation pathway, we created a U373-MG cell line with a tetracycline-repressible CA mutant of myosin light chain kinase (MLCK). Although graded activation of MLCK did not alter stress fiber or focal adhesion formation to the same extent as CA RhoA (Fig. S6), consistent with previous observations that MLCK-dependent stress fibers are largely limited to the cell periphery (21–23), CA MLCK expression did significantly increase cell-ECM traction forces (Fig. 3 *b*). To confirm that this effect was not simply an artifact of tetracycline treatment, we measured the traction forces of U373-MG control cells cultured with or without tetracycline, and found no significant difference (Fig. 3 *c*). Because traction stresses are known to be dependent on cell area and shape (24–27), we measured the area and perimeter of CA RhoA and CA MLCK cells during traction force experiments. We found that the cell area did not change significantly with tetracycline concentration, but the cells did adopt a less polarized morphology with increasing RhoA/MLCK activity (Fig. S7).

To demonstrate that we could also control intrinsic mechanical properties of the cells, we used AFM nanoindentation to measure cellular stiffness, which reflects the cell's shape plasticity and resistance to deformation. We found that increasing CA RhoA or MLCK expression in the U373-MG cell lines caused a graded increase in stiffness (Fig. 3 *d*), which could be prevented by treatment with blebbistatin (Fig. S8). The stiffness of control cells, on the other hand, did not increase with decreasing tetracycline concentration (Fig. 3 *d*). Plotting the traction force data (Fig. 3, *a* and *b*) against the stiffness data (Fig. 3 *d*) shows a strong correlation between traction force generation and cellular stiffness (Fig. 3, *e* and *f*), which is consistent with previous studies (8,27).

Cellular stiffness, traction force generation, and adhesion all represent isolated cellular properties that contribute to more complex cell behaviors that ultimately drive tissue function. To determine whether our approach could be

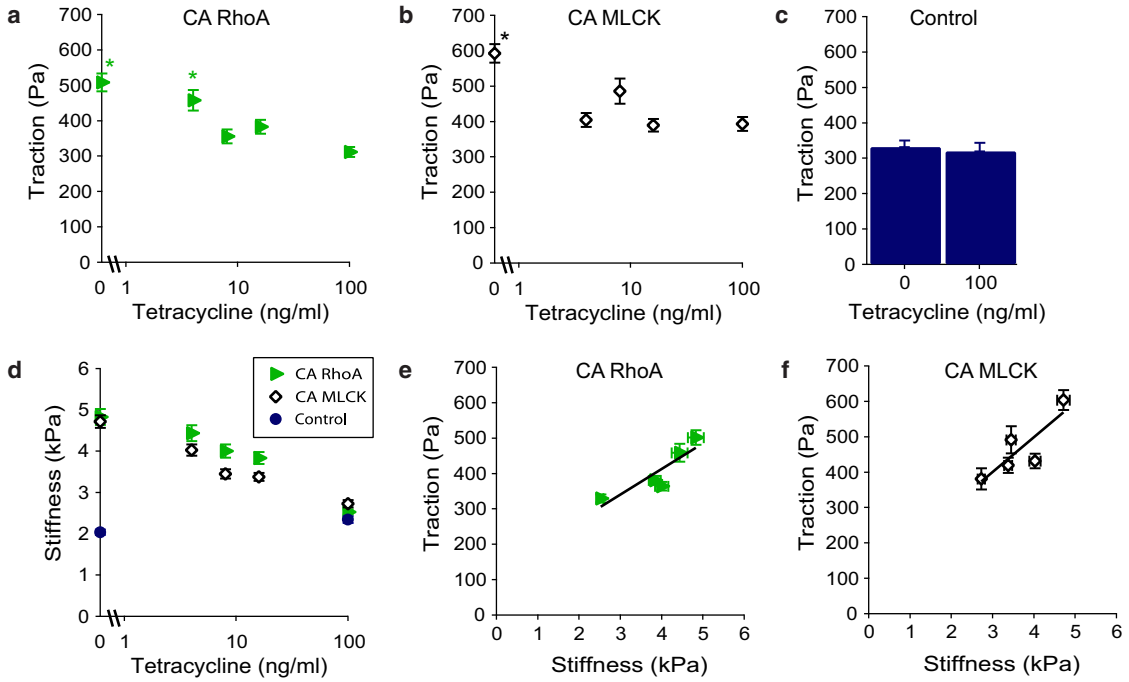

FIGURE 3 Graded increases in traction force generation and cortical stiffness with CA RhoA and MLCK expression. Average traction forces of U373-MG CA RhoA (*a*), CA MLCK (*b*), and control cells (*c*) were measured on polyacrylamide gels with elastic moduli of 8.8 kPa, 12.2 kPa, and 10.3 kPa, respectively. Mean ± SE ($n = 50$–105 cells per condition); *$p < 0.05$ compared with 100 ng/ml tetracycline (ANOVA, Tukey post-hoc test). (*d*) Average cortical stiffness of U373-MG CA RhoA, CA MLCK, and control cells as measured by AFM. Mean ± SE ($n = 350$–450 cells per condition); all values are significantly different from 100 ng/ml tetracycline ($p < 0.05$ by ANOVA, Tukey post-hoc test). (*e* and *f*) Average traction force plotted against stiffness for U373-MG CA RhoA (*e*) and CA MLCK cells (*f*). Pearson's correlation coefficient for fits = 0.89 and 0.84 for CA RhoA and CA MLCK, respectively.

used to modulate these higher-order behaviors, we focused on cell migration, which requires both shape plasticity for a cell to extend its leading edge forward and force generation to retract its trailing edge. We first performed a scratch wound migration assay, in which a monolayer of cells is observed as it migrates into an open space, on the U373. We found that increasing CA RhoA or MLCK expression reduced the migration speed of U373-MG cells in a graded fashion and, as expected, the migration speed of control cells was not affected by tetracycline concentration (Fig. 4 *a*). This decrease in migration speed with CA RhoA and MLCK expression is likely due to the combined effects of enhanced cell-ECM adhesion, increased intracellular tension, and stronger cell-cell contacts. To eliminate the confounding factor of cell-cell contact and to investigate whether CA RhoA expression alters the relationship between cell migration speed and ECM stiffness, we tracked the random migration of single cells on fibronectin-coated polyacrylamide gels of defined stiffness, ranging from 0.1 to 73 kPa. We found that the average cell migration speed generally decreased with increasing CA RhoA expression on all stiffnesses (Fig. 4 *b*), but the strength of this trend appeared strongest on the softest gels. To clearly portray this sensitivity to RhoA modulation as a function of ECM stiffness, we calculated the percent decrease in cell speed due to CA RhoA expression (no tetracycline) as compared with the 100 ng/ml tetracycline condition for each stiffness. This analysis revealed that the migration speed of cells is at least three times more sensitive to RhoA modulation on the two softer gels than on the three stiffer gels (Fig. 4 *c*). We also depicted this result in rosette plots by superimposing the trajectories of many single cells on each stiffness gel (Fig. 4 *d* and Fig. S9). A possible explanation for this dependence of RhoA sensitivity on ECM stiffness is that decreasing ECM stiffness reduces endogenous RhoA activity (14), which in turn sensitizes cells on soft ECMs to CA RhoA expression.

Given the increased sensitivity to RhoA modulation on soft polyacrylamide gels, we were interested in further exploring the relationships among RhoA/MLCK activation, force generation, and migration on another soft, but more complex and dynamic microenvironment: collagen I hydrogels. These hydrogels form fibrillar matrices that cells can contract and remodel. When U373-MG cells were cultured on 1 mg/ml collagen gels with the CA genes suppressed, the cells elongated, bundled the collagen, and used these bundles as contact guidance cues to migrate toward one another (Fig. 5 *a*, Fig. S10, and Movie S1). Increasing CA RhoA or MLCK expression, however, drastically inhibited cell spreading and migration (Fig. 5 *b* and Movie S2). Higher-magnification time-lapse videos showed that cells with high RhoA activity remained rounded and attempted

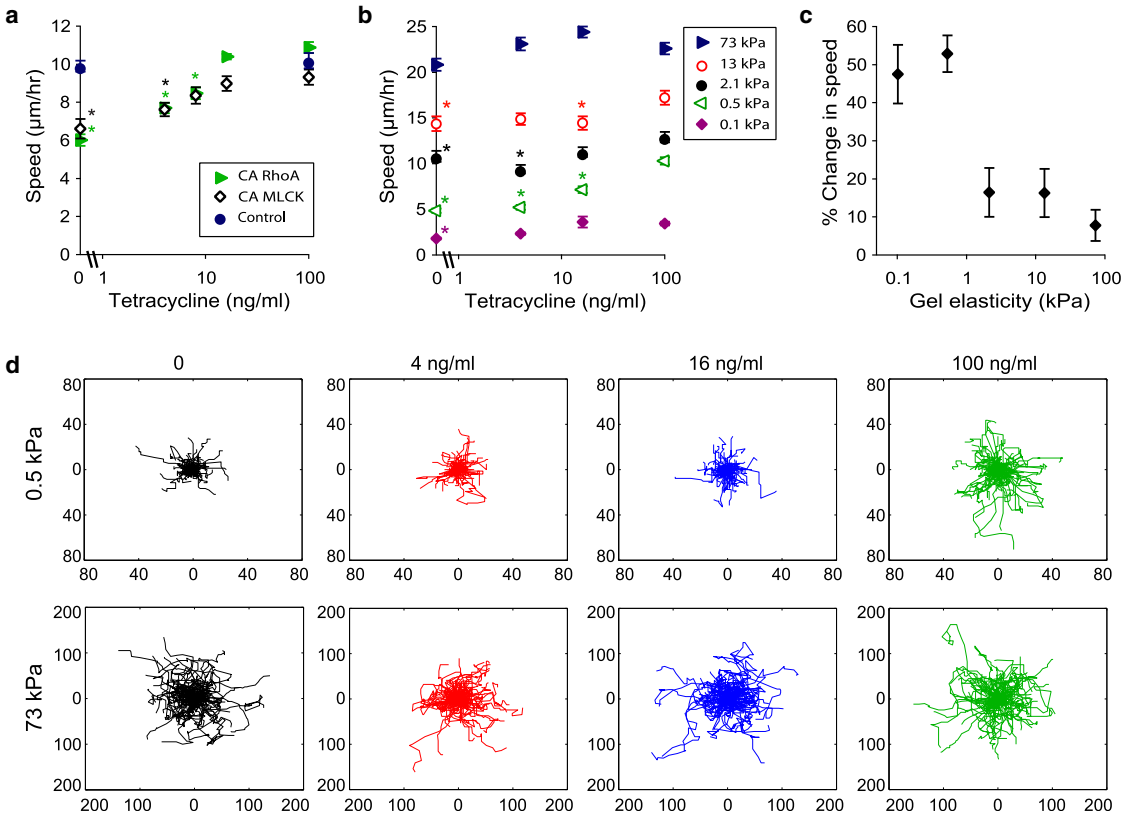

FIGURE 4 Graded decrease in migration speed with CA RhoA and MLCK expression. (*a*) Average migration speed of U373-MG CA RhoA, CA MLCK, and control cells during a scratch wound assay ($n = 8$–13 wells per condition). (*b*) Average migration speed of U373-MG CA RhoA cells cultured on polyacrylamide gels of defined stiffness ($n = 150$–350 cells per condition). For *a* and *b*, mean ± SE; $*p < 0.05$ compared with 100 ng/ml tetracycline (ANOVA, Tukey post-hoc test). (*c*) The percent decrease in migration speed due to CA RhoA expression was calculated from *b* on each stiffness by subtracting the no-tetracycline speed from the 100 ng/ml tetracycline speed, and then dividing by the 100 ng/ml tetracycline speed; mean ± SE. (*d*) Rosette plots depicting single cell trajectories from *b* on soft and stiff gels with varying tetracycline concentrations. Axes are in micrometers.

to engage the collagen matrix through weak, nascent adhesions (Movie S3), whereas cells with low RhoA activity were able to polarize and generate long-range tractional forces that facilitated cell migration (Movie S4). We were able to dynamically and reversibly switch between these two phenotypes by adding and withdrawing tetracycline (Fig. 5 *c*, Movie S5, and Movie S6). Consistent with our kinetic studies on GFP expression (Fig. 1 *f*), switching CA RhoA expression from off to on or vice versa began to alter cell spreading within 12–18 h. We next investigated our control over cell behavior in a three-dimensional collagen hydrogel by encapsulating U373-MG CA RhoA cells during gelation and measuring the degree to which cells contracted the gel over a day. We found that increasing CA RhoA expression reduced cellular contraction of the gel in a graded fashion almost twofold (Fig. 5 *d*), which is consistent with the idea that high RhoA-dependent intracellular contractility prevents cell spreading and therefore prevents cells from actively engaging and remodeling the ECM.

Finally, we compared the performance of this approach with that of analogous pharmacological interventions commonly used in the field. To our knowledge, no direct activators of RhoA and MLCK are currently available; therefore, we treated cells with varying concentrations of two pharmacological agents that should indirectly increase RhoA activity: lysophosphatidic acid (LPA), which engages G-protein-coupled receptors upstream of RhoA (28), and Rac1 inhibitor NSC23766, which would be expected to activate RhoA through Rho/Rac antagonism (29). To determine the effects of LPA and NSC23766 on stress fiber formation, we treated U373-MG control cells with each drug as a single bolus of defined dosage, and then fixed the cells after 5 min or 18 h. We found that LPA induced stress fiber formation within 5 min, but this effect largely dissipated after 18 h (Fig. S11). This is consistent with previous studies that showed that the effects of LPA are quite transient (30–32), presumably due to cellular sequestration and/or degradation of the drug. In addition, we found that LPA began to precipitate out of solution at 10 μM and 50 μM, reflecting its limited solubility in cell culture medium (33,34). In contrast, NSC23766 did not appear to significantly alter actin cytoarchitecture after 5 min, but it did enhance stress fiber formation and adoption of a less polarized morphology after 18 h (Fig. S11). During the longer incubation time,

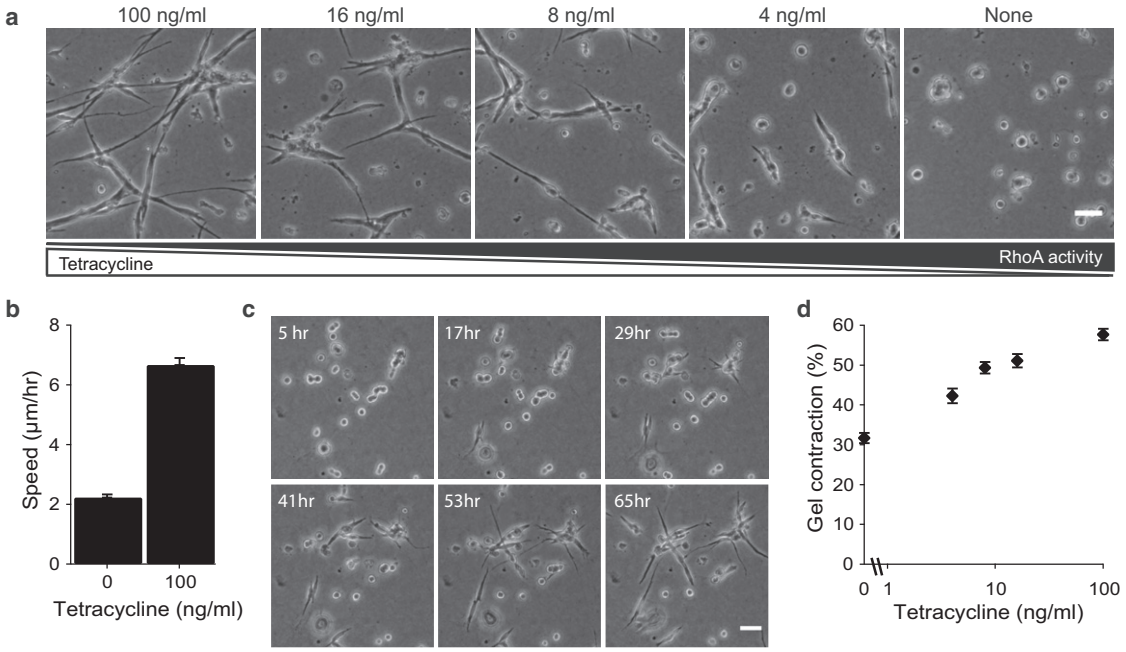

FIGURE 5 Graded and dynamic control over cell behavior on collagen hydrogels. U373-MG CA RhoA cells were cultured on top of 1 mg/ml collagen hydrogels (*a–c*) or suspended within them (*d*). (*a*) Micrographs of cells cultured on collagen gels with varying tetracycline concentrations. (*b*) Average migration speed of cells cultured with or without 100 ng/ml tetracycline. Mean ± SE ($n = 120$–130 cells per condition); $p < 0.001$ (Student's *t*-test). (*c*) Frames from Movie S5 in which cells were initially cultured without tetracycline and then switched to 100 ng/ml tetracycline at $t = 0$. (*d*) Percent decrease in gel area over 24 h during a 3D collagen contraction assay. Mean ± SE ($n = 6$ wells per condition); all values are significantly different from 100 ng/ml tetracycline ($p < 0.05$ by ANOVA, Tukey post-hoc test).

however, the highest concentration of NSC23766 caused widespread cell death. Incubation time also strongly influenced the effects of these drugs on cellular stiffness: whereas treatment with LPA or NSC23766 for 5 min significantly increased the stiffness of control cells, treatment for 18 h did not (Fig. 6, *a* and *b*). In addition, when we measured the migration speed of cells during a scratch wound assay conducted over 6 h (Fig. 6 *c*), we found that LPA treatment did not significantly alter cell migration speed, presumably because of LPA's limited period of bioactivity. The higher concentrations of NSC23766 significantly decreased the cell migration speed, but only at concentrations in which cell death was observed.

DISCUSSION

We have presented a genetic strategy for directly controlling the mechanobiological properties of living cells by regulating the expression of a single mutant gene from a repressible promoter. Our results show that with relatively low expression of CA RhoA (only 23% of endogenous RhoA; Fig. 1 *a*) or CA MLCK, we were able to induce graded

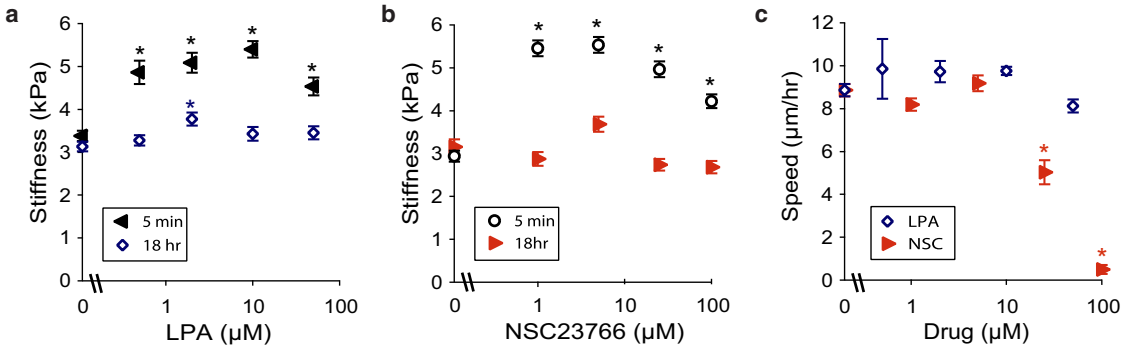

FIGURE 6 LPA and NSC23766 transiently increase cellular stiffness and do not significantly alter cell migration. (*a* and *b*) Average cortical stiffness of U373-MG control cells treated with LPA (*a*) and NSC23766 (*b*) at varying concentrations for 5 min or 18 h ($n = 135$–205 cells per condition). (*c*) Average migration speed of U373-MG control cells treated with LPA or NSC23766 at varying concentrations during a scratch wound migration assay ($n = 7$ wells per condition). Mean ± SE; *$p < 0.05$ compared with the no-drug condition (ANOVA, Tukey post-hoc test).

changes in stress fiber assembly (Fig. 2 *a*), cellular force generation (Fig. 3, *a* and *b*), cellular stiffness (Fig. 3 *d*), and migration speed (Fig. 4 *a* and *b*). We were also able to reversibly and dynamically control cell-ECM interactions on soft collagen hydrogels, including cell spreading, migration, and matrix remodeling (Fig. 5, Movie S1, Movie S2, Movie S3, Movie S4, Movie S5, and Movie S6). In addition to providing an important technical innovation, this approach enables us to gain several new insights into cell-ECM mechanobiology. First, we show that even though RhoA/ROCK and MLCK are known to regulate distinct pools of myosin II (21–23), these signaling systems produce similarly graded effects on cellular force generation, stiffness, and migration speed, and therefore may overlap significantly in their function. Second, we find that cells are maximally sensitive to perturbations in RhoA activity on soft ECMs (Fig. 4, *c* and *d*), presumably because soft ECMs suppress endogenous RhoA activation. Third, we directly expose several limitations to pharmacological activation of RhoA with LPA and NSC23766, including a short time window for altering cellular mechanical properties (<6–18 h; Fig. 6), the poor solubility of LPA in cell culture medium, and the high toxicity of NSC23766. Because our genetic approach does not suffer from these drawbacks and provides access to a wide range of timescales and protein activities, we envision that it will enable new investigations and manipulations of dynamic processes that occur over multiple days, such as stem cell lineage commitment, multicellular assembly, and matrix remodeling.

In this study, we varied the activity of two different types of protein (a GTPase and a kinase); however, the tetracycline-repressible construct potentially could be used to control any type of protein in any cell type. Because our goal was to obtain precise control over protein activity, we used retroviral gene delivery to introduce a single copy of CA RhoA or CA MLCK into cells and thereby limit the cell-to-cell variability that arises with high multiplicity of infections or plasmid transfection. A limitation of single-copy transduction is that protein expression is relatively low, which may require the expression of CA or dominant negative mutants to override endogenous feedback inhibition mechanisms and significantly alter total protein activity. Alternatively, several modifications could be applied to this system to increase gene expression. First, cells could be transduced at a higher multiplicity of infection and subsequently sorted by flow cytometry (based on GFP expression) to isolate cells with the same copy number. Second, the construct could be adapted for lentiviral gene delivery, which often yields higher transgene expression than retroviral systems. Third, the tetracycline-repressible promoter could be replaced with a stronger promoter system.

Our ability to vary RhoA and MLCK activity in a continuously graded fashion provides a unique opportunity to study the quantitative relationships between protein activity and cellular properties. For example, several studies have suggested that cell migration speed may depend biphasically on myosin activation, and that an intermediate level of activity is optimal for cell migration (10,35,36). We found that increasing RhoA/MLCK activity led to a graded decrease in migration speed (Fig. 4), presumably by causing cells to become too contractile or to adhere too strongly to the ECM. This leads us to wonder whether reducing RhoA/MLCK activity below endogenous levels would also hinder cell migration. With dominant negative or shRNA constructs, our genetic strategy may enable investigators to explore the effects of graded decreases in RhoA/MLCK activity and definitively determine whether a nonlinear relationship between myosin activity and cell migration actually exists.

Of importance, all of the mechanobiological properties we measured in this study change in a continuously graded fashion with graded increases in protein activity, as opposed to a bimodal (all or nothing) fashion. Because several key cell behaviors that traditionally have been considered to lie downstream of mechanotransductive signaling, such as proliferation and differentiation, are thought to be discrete endpoints that may be arrived at via a wide degeneracy of cellular signaling states (37), this in turn raises the question of how much signal activation is sufficient to produce a given phenotype. The strategy described here should put us in an excellent position to address these issues, and would be of particular interest when applied to stem cells and other developmental systems with a broad palette of phenotypic plasticity.

Finally, in addition to providing an experimental tool for investigating how small changes in mechanotransductive signaling translate to changes in cellular properties and behavior, our genetic strategy for precisely modulating the mechanical properties of cells could also serve as a powerful design handle for directly instructing cell function. We have shown that by inducing CA RhoA or MLCK expression, we can directly inhibit cell spreading on a collagen hydrogel and override physical cues from the matrix that would normally stimulate cell migration and clustering (Fig. 5 and Fig. S10). This suggests that cells can be genetically engineered to alter and control their responses to physical stimuli in their microenvironment, which could be particularly valuable in tissue engineering applications that interface cells with synthetic materials. The ability to precisely control cellular contractility and migration could also facilitate cellular actuation in various biotechnologies, such as cell-mediated delivery of therapeutics, and in combination with promoter systems that respond to physiologically relevant molecules (e.g., hormones and steroids), these technologies could serve a dual role as biosensors. Furthermore, by introducing specific populations of genetically engineered cells into animal models and administering transcriptional inducers or repressors systemically, this genetic approach could give investigators unique opportunities to study and control cellular mechanobiology in vivo.

SUPPORTING MATERIAL

Six movies and 11 figures are available at http://www.biophysj.org/biophysj/supplemental/S0006-3495(12)00037-9.

We thank D. V. Schaffer for providing valuable technical guidance and sharing equipment, and R. A. Segalman for providing access to the atomic force microscope. We also thank B. Sandhu for her help in characterizing the U373-MG CA MLCK cell line. Confocal images were obtained at the CIRM/QB3 Stem Cell Shared Facility.

This work was supported by grants to S.K. from the National Science Foundation (NSF CMMI 0727420, CMMI 1055965, and CMMI 1105539) and the National Institutes of Health (1DP2OD004213, Director's New Innovator Award, NIH Roadmap for Medical Research; 1U54CA143836, Physical Sciences Oncology Center Grant). J.L.M. was supported in part by a Graduate Research Supplement to Broaden Participation, in association with NSF CMMI 0727420. A.J.K. was supported by a National Defense Science and Engineering graduate fellowship and an NSF graduate research fellowship.

REFERENCES

1. Ingber, D. E. 2003. Mechanobiology and diseases of mechanotransduction. *Ann. Med.* 35:564–577.
2. Jaalouk, D. E., and J. Lammerding. 2009. Mechanotransduction gone awry. *Nat. Rev. Mol. Cell Biol.* 10:63–73.
3. Kumar, S., and V. M. Weaver. 2009. Mechanics, malignancy, and metastasis: the force journey of a tumor cell. *Cancer Metastasis Rev.* 28:113–127.
4. Chen, C. S., M. Mrksich, …, D. E. Ingber. 1997. Geometric control of cell life and death. *Science.* 276:1425–1428.
5. Wang, H. B., M. Dembo, and Y. L. Wang. 2000. Substrate flexibility regulates growth and apoptosis of normal but not transformed cells. *Am. J. Physiol. Cell Physiol.* 279:C1345–C1350.
6. Discher, D. E., P. Janmey, and Y. L. Wang. 2005. Tissue cells feel and respond to the stiffness of their substrate. *Science.* 310:1139–1143.
7. Vogel, V., and M. Sheetz. 2006. Local force and geometry sensing regulate cell functions. *Nat. Rev. Mol. Cell Biol.* 7:265–275.
8. Wang, N., I. M. Tolić-Nørrelykke, …, D. Stamenović. 2002. Cell prestress. I. Stiffness and prestress are closely associated in adherent contractile cells. *Am. J. Physiol. Cell Physiol.* 282:C606–C616.
9. Wakatsuki, T., R. B. Wysolmerski, and E. L. Elson. 2003. Mechanics of cell spreading: role of myosin II. *J. Cell Sci.* 116:1617–1625.
10. Salhia, B., J. H. Hwang, …, J. T. Rutka. 2008. Role of myosin II activity and the regulation of myosin light chain phosphorylation in astrocytomas. *Cell Motil. Cytoskeleton.* 65:12–24.
11. Beadle, C., M. C. Assanah, …, P. Canoll. 2008. The role of myosin II in glioma invasion of the brain. *Mol. Biol. Cell.* 19:3357–3368.
12. Mitrossilis, D., J. Fouchard, …, A. Asnacios. 2009. Single-cell response to stiffness exhibits muscle-like behavior. *Proc. Natl. Acad. Sci. USA.* 106:18243–18248.
13. Gallagher, P. J., B. P. Herring, …, J. T. Stull. 1993. A molecular mechanism for autoinhibition of myosin light chain kinases. *J. Biol. Chem.* 268:26578–26582.
14. Keung, A. J., E. M. de Juan-Pardo, …, S. Kumar. 2011. Rho GTPases mediate the mechanosensitive lineage commitment of neural stem cells. *Stem Cells.* 29:1886–1897.
15. Butler, J. P., I. M. Tolić-Nørrelykke, …, J. J. Fredberg. 2002. Traction fields, moments, and strain energy that cells exert on their surroundings. *Am. J. Physiol. Cell Physiol.* 282:C595–C605.
16. Bilodeau, G. G. 1992. Regular pyramid punch problem. *J. Appl. Mech.* 59:519–523.
17. Ridley, A. J. 1997. The GTP-binding protein Rho. *Int. J. Biochem. Cell Biol.* 29:1225–1229.
18. Ulrich, T. A., E. M. de Juan Pardo, and S. Kumar. 2009. The mechanical rigidity of the extracellular matrix regulates the structure, motility, and proliferation of glioma cells. *Cancer Res.* 69:4167–4174.
19. Sen, S., M. Dong, and S. Kumar. 2009. Isoform-specific contributions of α-actinin to glioma cell mechanobiology. *PLoS ONE.* 4:e8427.
20. Fukata, M., and K. Kaibuchi. 2001. Rho-family GTPases in cadherin-mediated cell-cell adhesion. *Nat. Rev. Mol. Cell Biol.* 2:887–897.
21. Totsukawa, G., Y. Yamakita, …, F. Matsumura. 2000. Distinct roles of ROCK (Rho-kinase) and MLCK in spatial regulation of MLC phosphorylation for assembly of stress fibers and focal adhesions in 3T3 fibroblasts. *J. Cell Biol.* 150:797–806.
22. Katoh, K., Y. Kano, …, K. Fujiwara. 2001. Stress fiber organization regulated by MLCK and Rho-kinase in cultured human fibroblasts. *Am. J. Physiol. Cell Physiol.* 280:C1669–C1679.
23. Tanner, K., A. Boudreau, …, S. Kumar. 2010. Dissecting regional variations in stress fiber mechanics in living cells with laser nanosurgery. *Biophys. J.* 99:2775–2783.
24. Wang, N., E. Ostuni, …, D. E. Ingber. 2002. Micropatterning tractional forces in living cells. *Cell Motil. Cytoskeleton.* 52:97–106.
25. Li, F., B. Li, …, J. H. Wang. 2008. Cell shape regulates collagen type I expression in human tendon fibroblasts. *Cell Motil. Cytoskeleton.* 65:332–341.
26. Rape, A. D., W. H. Guo, and Y. L. Wang. 2011. The regulation of traction force in relation to cell shape and focal adhesions. *Biomaterials.* 32:2043–2051.
27. Tee, S. Y., J. Fu, …, P. A. Janmey. 2011. Cell shape and substrate rigidity both regulate cell stiffness. *Biophys. J.* 100:L25–L27.
28. Moolenaar, W. H. 1999. Bioactive lysophospholipids and their G protein-coupled receptors. *Exp. Cell Res.* 253:230–238.
29. Guilluy, C., R. Garcia-Mata, and K. Burridge. 2011. Rho protein crosstalk: another social network? *Trends Cell Biol.* 21:718–726.
30. Ren, X. D., W. B. Kiosses, and M. A. Schwartz. 1999. Regulation of the small GTP-binding protein Rho by cell adhesion and the cytoskeleton. *EMBO J.* 18:578–585.
31. van Nieuw Amerongen, G. P., M. A. Vermeer, and V. W. van Hinsbergh. 2000. Role of RhoA and Rho kinase in lysophosphatidic acid-induced endothelial barrier dysfunction. *Arterioscler. Thromb. Vasc. Biol.* 20:E127–E133.
32. Van Leeuwen, F. N., C. Olivo, …, W. H. Moolenaar. 2003. Rac activation by lysophosphatidic acid LPA1 receptors through the guanine nucleotide exchange factor Tiam1. *J. Biol. Chem.* 278:400–406.
33. Möller, T., J. J. Contos, …, B. R. Ransom. 2001. Expression and function of lysophosphatidic acid receptors in cultured rodent microglial cells. *J. Biol. Chem.* 276:25946–25952.
34. Durieux, M. E., S. J. Carlisle, …, K. R. Lynch. 1993. Responses to sphingosine-1-phosphate in *X. laevis* oocytes: similarities with lysophosphatidic acid signaling. *Am. J. Physiol.* 264:C1360–C1364.
35. Wilson, A. K., G. Gorgas, …, P. de Lanerolle. 1991. An increase or a decrease in myosin II phosphorylation inhibits macrophage motility. *J. Cell Biol.* 114:277–283.
36. Gupton, S. L., and C. M. Waterman-Storer. 2006. Spatiotemporal feedback between actomyosin and focal-adhesion systems optimizes rapid cell migration. *Cell.* 125:1361–1374.
37. Huang, S., G. Eichler, …, D. E. Ingber. 2005. Cell fates as high-dimensional attractor states of a complex gene regulatory network. *Phys. Rev. Lett.* 94:128701.